JOURNAL OF GEOPHYSICAL RESEARCH, VOL. 113, C10011, doi:10.1029/2007JC004582, 2008

Estimating sea ice area flux across the Canadian Arctic Archipelago using enhanced AMSR-E

T. Agnew,[1] A. Lambe,[2] and D. Long[3]

Received 16 October 2007; revised 23 June 2008; accepted 25 July 2008; published 15 October 2008.

[1] Enhanced resolution Advanced Microwave Scanning Radiometer (AMSR-E) imagery is used to estimate daily sea ice area fluxes between the Canadian Arctic Archipelago and the Arctic Ocean and Baffin Bay for the period September 2002 to June 2007. Over the period, Amundsen Gulf and M'Clure Strait exported 54×10^3 km^2 of sea ice area or roughly 77 km^3 of sea ice volume each year into the Arctic Ocean. Export/import into the Arctic Ocean through the Queen Elizabeth Islands is small and uncertain since no estimates for July and August could be made due to atmospheric attenuation of the microwave signal. Lancaster Sound exported 68×10^3 km^2 of sea ice area or roughly 102 km^3 of ice volume into Baffin Bay. This produced a net loss of sea ice area of about 122×10^3 km^2 or roughly 174 km^3 a^{-1} which is presumed to be generated from within the Archipelago itself mainly through the stationary and transient polynyas and leads that form each winter. Daily ice area fluxes for Amundsen Gulf (AG) and Lancaster Sound (LS) were as high as ±2500 km^2 d^{-1} and were event driven depending on synoptic scale atmospheric circulation and the mobility of the sea ice. Mean sea level pressure difference across each gate is moderately correlated with daily sea ice area fluxes despite the fact that free ice drift conditions are not always met in the region. Cross-gradient and daily sea ice area flux for Lancaster Sound show a large number of counter gradient ice flux occurrences suggesting that local mesoscale winds (nongeostrophic) and perhaps ocean currents play a role in transporting sea ice through this gate. Monthly ice fluxes for the AG and MS gate were positively correlated with the AO index indicating that a strong Beaufort Sea high pressure and gyre correspond to more export into the Beaufort Sea. Monthly fluxes for the LS gate were positively correlated with the NAO index indicating that strong southerly atmospheric circulation over Baffin Bay increases ice export into Baffin Bay from Lancaster Sound.

Citation: Agnew, T., A. Lambe, and D. Long (2008), Estimating sea ice area flux across the Canadian Arctic Archipelago using enhanced AMSR-E, *J. Geophys. Res.*, *113*, C10011, doi:10.1029/2007JC004582.

1. Introduction

[2] The Canadian Arctic Archipelago (CAA) is a collection of islands and channels in the most northern part of Canada facing the Arctic Ocean to the north and west and Baffin Bay to the east (Figure 1). Sea ice persists within the CAA throughout the year, although regions to the south and east usually clear by late summer. Freezeup begins in October and ice within the Archipelago consolidates by mid to late winter, although stationary and transient polynyas and leads form during the winter creating large amounts of new ice [*Smith et al.*, 1990]. A summary of the oceanography, sea ice and climate conditions for the region is provided by *Melling* [2002] and *Melling et al.* [2008]. With the increased evidence for Arctic warming and recent large reductions in sea ice cover [*Meier et al.*, 2007; *Stroeve et al.*, 2007; *Ngheim et al.*, 2006], there is increased interest in the Archipelago as a possible Northwest Passage between Europe and Asia in summer [*Wilson et al.*, 2004]. The region is also important as a pathway of freshwater flux via the Pacific/Arctic Ocean into Baffin Bay [*Jones et al.*, 2003].

[3] *Kwok* [2006] estimated the sea ice flux between the Arctic Ocean and the Archipelago using RADARSAT imagery during the period (1997 to 2002) prior to the launch of AMSR-E and the period of this study. He found a net export of sea ice into the Arctic Ocean of 85×10^3 km^2. *Howell et al.* [2008] summarized changing multiyear ice (MYI) conditions using Canadian Ice Services ice charts and provided evidence that MYI forms within the western and northern parts of the Archipelago and slowly migrates southeast. *Alt et al.* [2006] documented the import and export of old ice through the Peary and Sverdrup Channels following the record low ice cover in 1998.

[1]Environment Canada, Toronto, Ontario, Canada.
[2]Faculty of Applied Science and Engineering, University of Toronto, Toronto, Ontario, Canada.
[3]Microwave Earth Remote Sensing Laboratory, Brigham Young University, Provo, Utah, USA.

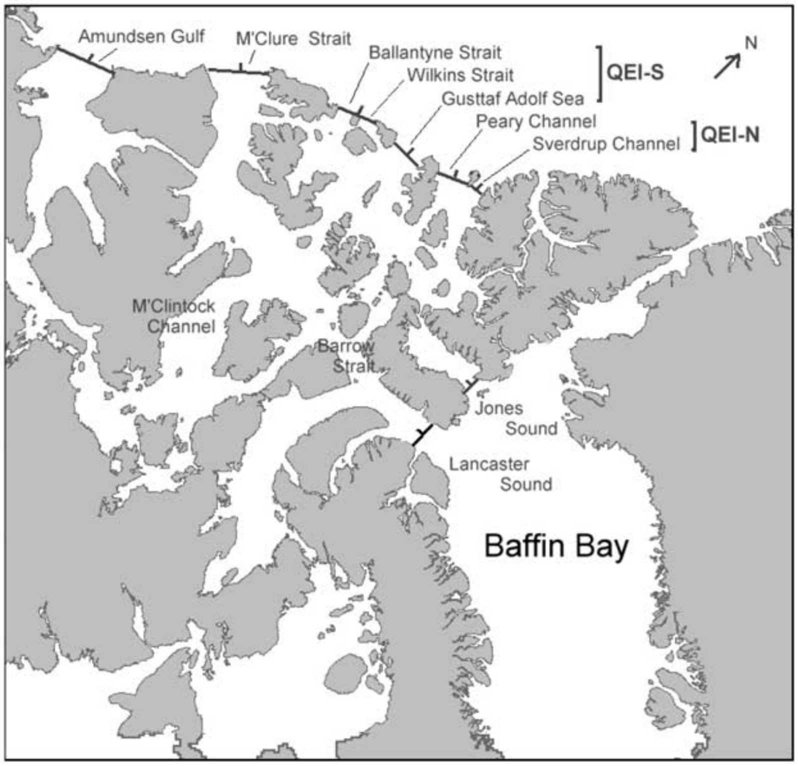

Figure 1. Location and name of each fluxgate: Amundsen Gulf (AG), M'Clure Strait (MS), Queen Elizabeth Islands South (QEI-S), Queen Elizabeth Islands North (QEI-N), Jones Sound (JS), and Lancaster Sound (LS).

[4] The flux of sea ice into Baffin Bay is through Lancaster Sound and Jones Sound (Figure 1). Both these channels have permanent winter polynyas near the entrance to Baffin Bay producing newly formed sea ice which is then transported into Baffin Bay. *Marko* [1982] estimated 75 km^3 of sea ice is created each winter from the Lancaster Sound polynya. *Kwok* [2007] used AMSR-E data over the same period of this study to estimate ice drift in Baffin Bay and although he did not estimate the export of sea ice from the Archipelago into Baffin Bay, his results suggested that about one third of the 530×10^3 km^2 of ice area transported south in Baffin Bay comes from Lancaster Sound and Jones Sound and the north open water polynya in the very northern part of the Bay.

[5] *Kwok* [2007] compared sea ice motion from non-enhanced AMSR-E imagery and Envisat SAR data in northern Baffin Bay. He found that AMSR-E ice motion accounted for about 90% of the variance in the smoothed Envisat ice motions. This paper estimates daily sea ice motion and sea ice area flux between the Archipelago and the Arctic Ocean and Baffin Bay for the period September 2002 through to June 2007 using AMSR-E data which is spatially enhanced using Scatterometer Image Reconstruction [*Long and Daum*, 1998].

2. Data/Methods

[6] Mean sea level pressure data was obtained from the Global Environmental Multiscale (GEM) model (the operational weather model used in the Canadian Meteorological Centre) and Arctic Buoy data from the International Arctic Buoy Program (IABP) (http://iabp.apl.washington.edu). The nonenhanced AMSR-E data was obtained from the National Snow and Ice Data Center (http://nsidc.org/data/amsre/; http://www.nsidc.org/%7Eimswww/pub/imswelcome/index.html) and the resolution enhanced AMSR-E data was obtained from Brigham Young University (BYU), Microwave Earth Remote Sensing Laboratory (ftp://ftp.scp.byu.edu/pub/data/amsre/). Scatterometer Image Reconstruction (SIR) [*Long and Daum*, 1998] is used to spatially enhance the AMSR-E imagery. At 89 GHz, the pixel resolution of this enhanced imagery is approximately 2.2 km, which allows the estimate of ice motion in the main channels of the Archipelago. The SIR technique uses knowledge of the scan geometry and antenna pattern of the AMSR-E instrument to increase the effective resolution of the data. Multiple estimates of radiances from different orbits reduce pixel noise.

[7] Maximum cross correlation between two images separated one day apart is used to estimate sea ice motion [*Agnew et al.*, 1997; *Kwok et al.*, 1998]. The technique uses a 6×6 pixel search window and the maximum correlation in the search window between the two images determines the sea ice displacement. This produces an independent estimate of ice motion approximately every 13.5 km. The underlying premise is that differences between consecutive images result from a simple displacement, the same for all features. For images separated by a day, this assumption is reasonable. Sea ice concentrations were estimated from the 18.7 and 36.5 GHz channels of the AMSR-E sensor using the NASA Team algorithm [*Cavalieri and Crawford*, 1991].

Table 1. Comparison Between Nonenhanced and Enhanced AMSR-E Using Over 800 Arctic Drifting Buoy 1-Day Ice Motions[a]

Observations	Mean Difference	Standard Deviation	Mean Motion of Buoys
Enhanced AMSR-E	−0.40	3.27	7.03
Nonenhanced AMSR-E	−0.49	4.64	7.03

[a]Units are in km d^{-1}.

[8] To evaluate the accuracy of the enhanced AMSR-E ice motion estimates, they were compared with International Arctic buoy drift data over the western Arctic Ocean. Unfortunately, no Arctic buoys passed through the CAA during this period and so motion estimates were compared to buoys in the western Arctic north the Archipelago and in the Canada Basin. Because resolution enhancement of AMSR-E imagery tends to amplify noise [*Early and Long*, 2001] and can affect the correlation and ice motion estimates, ice motion from both enhanced and nonenhanced AMSR-E imagery were compared. Table 1 shows the standard deviation of the difference (imagery minus buoy) to be higher for nonenhanced AMSR-E imagery indicating that any increased noise in the enhanced AMSR-E imagery is offset by the improved spatial resolution.

[9] The location of the fluxgates used in this study to estimate sea ice flux is shown in Figure 1. The Amundsen Gulf gate (AG) extends 180 km from Cape Bathurst Peninsula to Sachs Harbour on the south side of Banks Island. The M'Clure Strait gate (MS) extends 180 km from the northern side of Banks Island to southern coast of Prince Patrick Island. The Queen Elizabeth Island south gate (QEI-S) consists of three gates across Ballantyne Strait (45 km wide), Wilkins Strait (35 km wide) and Prince Gustaf Adolf Sea (95 km wide). The Queen Elizabeth Island north gate (QEI-N) consists of two smaller gates extending across the entrance to Peary Channel (90 km) and Sverdrup Channel (45 km). These gates cover the exchange of sea ice with the Arctic Ocean and are close to the locations of the gates used by *Kwok* [2006] to estimate ice area flux using RADARSAT for the earlier 1997 to 2002 period.

[10] The Lancaster Sound gate (LS) extends 75 km across Lancaster Sound from the Bordon Peninsula of Baffin Island directly north to the southern shore of Devon Island. The sound is usually ice-free from June to September. The magnitude of tidal motion in the sound can be large. *Prinsenberg and Hamilton* [2005] estimate the motion to be around 4 km/d. Since the tidal frequencies are not exactly 24 h, there is a shift in displacement from day to day (the equivalent of a few hours). This will effect the ice displacement between daily AMSR-E images; however, this effect is small compared to the resolution of the AMSR-E imagery and is ignored. The Jones Sound (JS) gate extends 45 km from Belcher Point on Devon Island to King Edward Point on Ellesmere Island. Ice flux in the direction of the normal to each fluxgate shown in Figure 1 is negative. For the gates facing the Arctic Ocean, negative flux means export of sea ice into the Arctic Ocean. For the gates facing Baffin Bay, positive flux means export of sea ice into Baffin Bay.

[11] The enhanced AMSR-E data had occasional missing pixels due to binning of swath data onto the polar grid. These missing pixels were filled in using the median of the nearest 8 neighbors. High atmospheric moisture in summer prevents using the 89 GHz channel in July and August for estimating sea ice motion and sea ice area flux. This results in an uncertainty in the annual sea ice area flux for the MS, QEI-S and the QEI-N gates. All the other gates are ice free during July and August.

[12] Both ice concentration and ice motion are interpolated to a 10 km grid and then to locations along each fluxgate. The ice motion normal to each gate is interpolated to locations spaced approximately 10 km apart along the gate. The sea ice area flux (F) across each gate is calculated as follows:

$$F = \sum c_i u_i \Delta x$$

where Δx is the spacing of flux estimates along the gate, u_i is the ice motion normal to the fluxgate at the ith location, and c_i is the sea ice concentration. Occasional missing days and/or orbits in the AMSR-E images resulted in no daily flux estimate. Area flux during these missing days was estimated using the average daily flux for that month. This occurred no more than four times in any given month except for the period 14–30 December 2003 when the AMSR-E sensor was shut down during a particularly strong solar flare event.

[13] The error in estimating sea ice area flux depends on the accuracy of ice motion and sea ice concentration estimates. The comparison of enhanced AMSR-E ice motions with drifting buoys indicate an ice motion error of 3.27 km/d (Table 1) and the accuracy in estimating sea ice concentration is 10% [*Cavalieri et al.*, 1999]. Assuming these two sources of error are uncorrelated, the error (σ_e) in estimating the ice area flux element c_i u_i across a one km wide gate is 3.35 km^2/d. The number of independent ice flux estimates along the gate is determined by the size of the search window used to obtain independent ice motion estimates (6 pixels $\times$ 2.2 km $\sim$ 13.5 km) and the length of the gate (L). For Amundsen Gulf (AG) as an example, there are about 180 km/(13.5 km) $\sim$ 13 independent

Table 2. Gate Length and Sea Ice Area Flux Error Estimates for Each Gate

Gate Name	Gate Symbol	L (km)	σ_f (day) (km^2)	σ_f (month) (10^3 km^2)	σ_f (10 months) (10^3 km^2)
Amundsen Gulf	AG	180	163	0.9	2.5
M'Clure Strait	MS	180	163	0.9	2.5
QEI South	QEI-S	180	163	0.9	2.5
QEI North	QEI-N	135	144	0.8	2.2
Lancaster Sound	LS	75	105	0.6	1.6
Jones Sound	JS	45	80	0.4	1.3

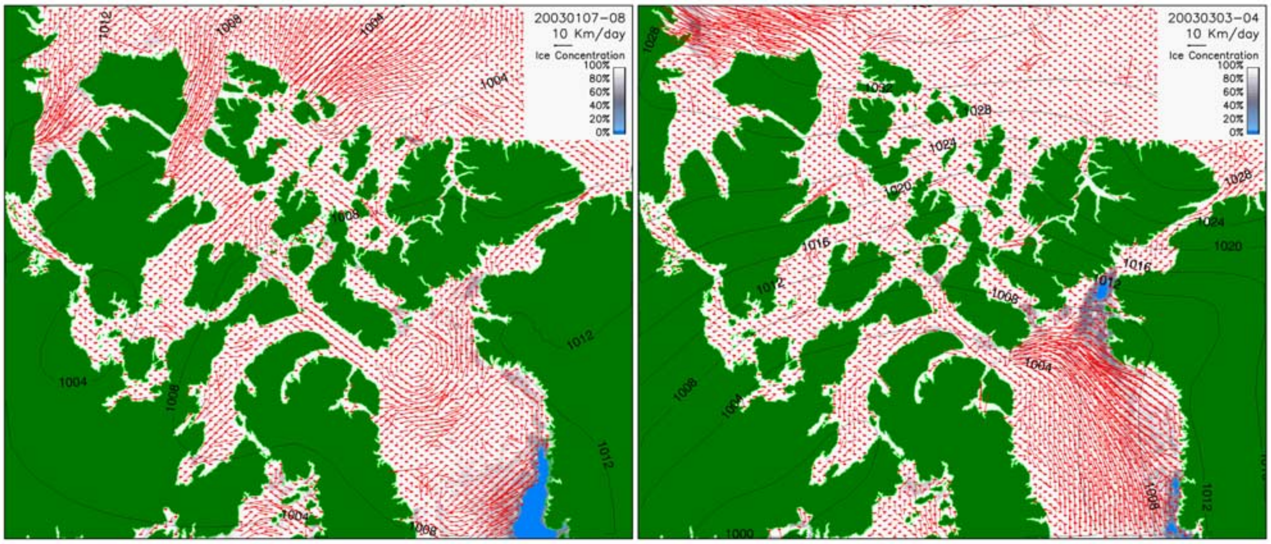

Figure 2. Daily sea ice motion for 7-8 January and 3-4 March 2003. Vectors are displayed with a dot indicating the location and beginning of the motion and a line indicating the direction and magnitude. Sea ice concentration estimated using the NT algorithm and mean sea level pressure are also shown.

estimates of ice flux (Ns). We assume that the errors in the individual fluxes sampled are additive, unbiased, uncorrelated, and normally distributed. Then, the uncertainty in the daily ice motion across the gate is $\sigma_f = \sigma_e \, L/(N_s)^{1/2}$. Uncertainty in the average monthly flux is $\sigma_T = \sigma_f \, (N_d)^{1/2}$ where N_d is the number of days in the month. For each gate the error estimate in the daily ice area flux, monthly ice area flux (30 days) and the 10-month ice area flux (September to June) are summarized in Table 2. As part of the quality control, daily 89 GHz horizontal channel images for the Archipelago region were made and animated. These animations were then used as a visual check on the ice flux estimates for individual days and gates.

[14] Estimating sea ice volume flux requires ice thickness measurements across each gate on a daily basis corresponding to the daily ice area flux estimates. This is not available. A very approximate estimate of ice thickness can be obtained using proxy estimates of ice thickness from borehole measurements, moored or submarine upward looking sonar or general knowledge of ice type in the area of each gate. However, these rough volume estimates are only a guide since the correlation between ice motion and ice thickness is ignored and the ice thickness estimate is uncertain. With the launch of ICESat's Geoscience Laser Altimeter System, several studies have looked into estimating sea ice thickness from space [*Kwok et al.*, 2007; *Spreen et al.*, 2006]. Although these studies are promising, the methods are still in development. ICESat repeat coverage for this region is only about 30 days and further research is needed to account for snow depth and density to come up with a more accurate estimate of sea ice freeboard.

3. Results

3.1. Daily Ice Motion, Ice Area Flux, and Cross-Gradient Flux Relationship

[15] Figure 2 shows daily sea ice motion estimates for two periods: 7–8 January and 3–4 March 2003. Ice motion vectors are displayed with a dot indicating the location and beginning of the motion and a line indicating the direction and magnitude. These vectors are overlayed on the sea ice concentration estimated using the NASA team (NT) algorithm [*Cavalieri and Crawford*, 1991]. Also shown is the mean sea level pressure from the Canadian Meteorological Centre analysis. The 7–8 January period shows sea ice imported into the Archipelago from the gates facing the Arctic Ocean especially the AG, MS and QEI-S (Prince Gustaf Adolf Sea) gates. Ice motion into M'Clure Strait ranges between 10 to 15 km/d. At this time sea ice in the interior channels is largely unconsolidated and there are smaller ice motions in M'Clintock Channel and Barrow Strait. Sea ice also enters the Archipelago from Lancaster Sound. The eastern part of the Archipelago including Lancaster Sound has higher more rugged terrain and orographically channeled winds and ocean currents play an important role in this region of the Archipelago [*Samelson et al.*, 2006]. Cyclonic ice motion is seen in northern Baffin Bay and is a common occurrence as noted by *Kwok* [2007]. The second period for 7–8 March 2003 shows a strong surface pressure gradient over the region with sea ice export out of M'Clure Strait into the Arctic Ocean, strong anticyclonic ice motion off Banks Island, and large ice motion parallel to Amundsen Gulf gate. By this time in late winter, most of the ice in the central part of the Archipelago has consolidated resulting in little or no motion despite the strong pressure gradient over the region. Lancaster Sound, however, remains unconsolidated downstream from the ice bridge which has formed in Barrow Strait. Ice motion in Lancaster Sound is westward into the Archipelago (negative) becoming more variable toward Baffin Bay. Motion in northern Baffin Bay is strongly westward and cyclonic with speeds up to 15 km/d under the influence of a strong pressure gradient. The low ice concentrations in the North Open Water (NOW) polynya are also seen.

[16] The time series of daily ice area flux over the 5-year period for each gate is shown in Figures 3a–3c. Area fluxes

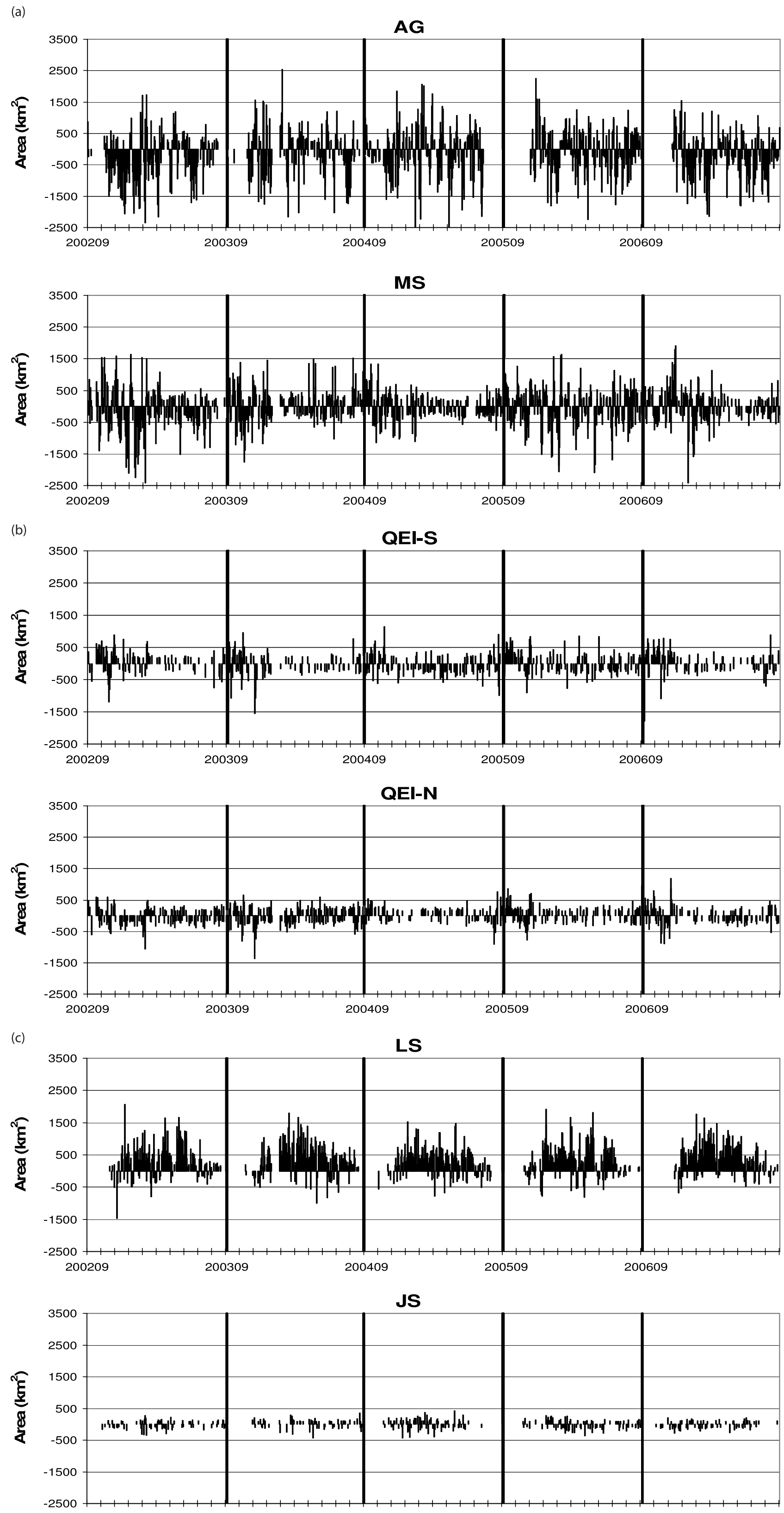

Figure 3. (a) Daily sea ice area fluxes for AG and MS gates. (b) Daily sea ice area fluxes for QEI-S and QEI-N gates. (c) Daily sea ice area fluxes for LS and JS gates.

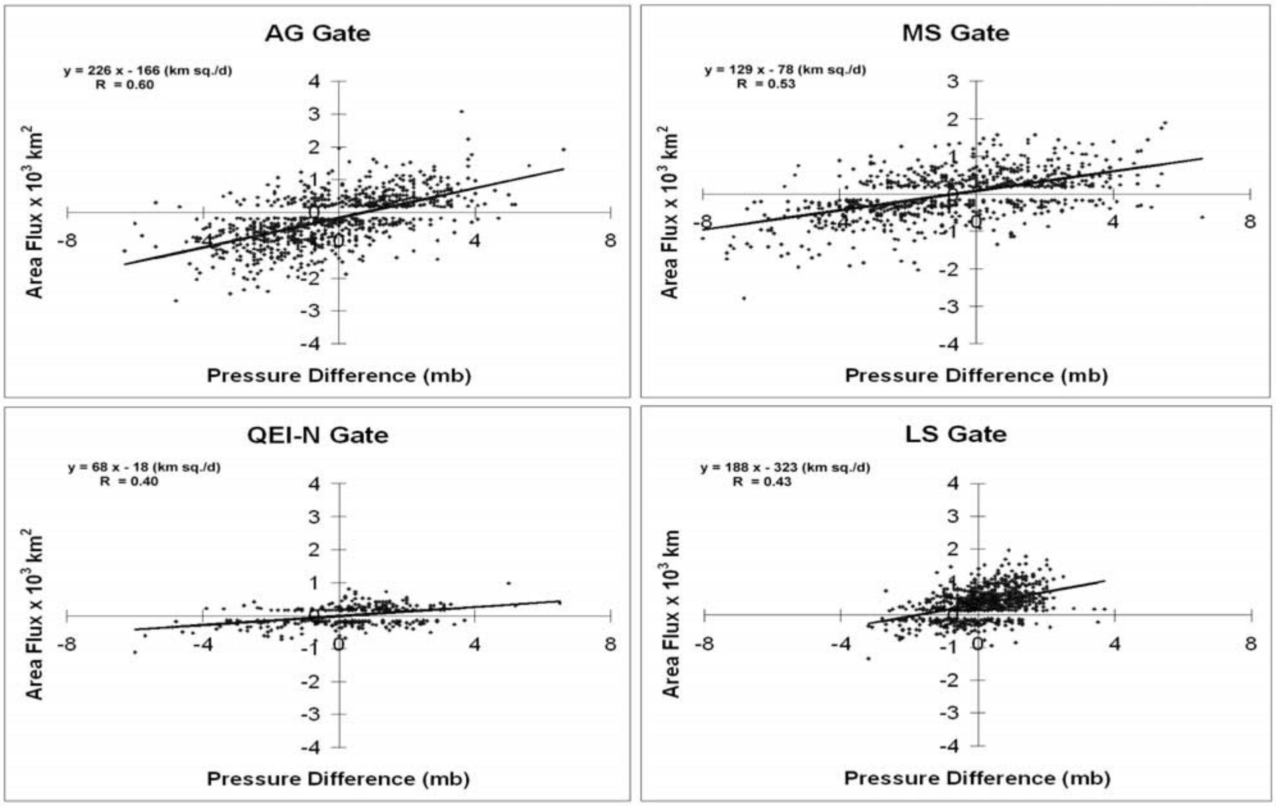

Figure 4. Scatterplot of daily fluxes and cross gate pressure differences for AG gate, MS gate, QEI-N gate, and LS gate.

less than the estimated flux error (Table 2) are not plotted since they are below the error estimate for each gate. For the four gates facing the Arctic Ocean (AG, MS, QEI-S and QEI-N) negative ice area flux corresponds to ice export into the Arctic Ocean. The largest daily fluxes and flux variability occurs through AG and MS gates. Daily area fluxes as large as ±2500 km^2 pass through the AG gate and negative fluxes are more frequent suggesting a net export into the Beaufort Sea. Area fluxes through the MS gate are slightly smaller. Periods of negative or positive flux last for several days to one week or more and are the result of large scale synoptic systems which pass through the region. Ice exchange across these two gates happens throughout the winter but reduces in late winter (February to April). Exchange across the QEI-S and QEI-N gates (Figure 3b) is smaller and less frequent with a suggestion that most of the exchange occurs in late fall to early winter (September to December). Of the two gates facing Baffin Bay, the LS gate exports by far the most ice into Baffin Bay with a preponderance of large positive daily ice fluxes (Figure 3c). Most of these events transport recently formed thin first year ice generated downstream of the ice bridge and polynya which forms each winter.

[17] Ice motion under free drift conditions is mainly wind driven and parallel to the sea level pressure isobars [*Thorndike and Colony*, 1982]. The response of daily sea ice fluxes to the cross gate pressure gradient was investigated by defining the mean sea level (msl) pressure difference between the two ends of each fluxgate. The gradient difference across each gate is positive/negative corresponding to positive/negative flux direction across each gate. Figure 4 shows scatterplots of pressure difference across each gate and ice area flux. QEI-S (not shown) was similar to QEI-N and the JS gate (not shown) had no correlation. The cross pressure difference is a fair predictor of flux and the correlations range from 0.60 for the AG gate to 0.40 for the QEI-N gate. These correlations are significantly different from zero at the $p = 0.05$ level. Within the Archipelago near these gates, internal ice stresses caused by local sea ice interaction can be large and free ice drift conditions will not always exist. The difference in regression slope between AG, MS and QEI-N gates is an indication of this. The AG slope is twice the slope for the MS gate and over three times the slope of the QEI-N gate indicating that ice through the AG gate is thinner and/or closer to free ice drift conditions compared to the MS and QEI-N gates. The slope of the LS gate is between the AG and MS values indicating thinner ice but the correlation is lower. For the LS gate, there are a large number of positive ice fluxes indicating net export into Baffin Bay but also a large percentage of points in the second quadrant indicating frequent counter gradient ice motion. This suggests that local mesoscale winds (non-geostrophic) and perhaps ocean currents play a role in transporting sea ice through this gate.

3.2. Typical Monthly Pattern of Ice Motion in the Archipelago

[18] Figures 5a–5e show the monthly average sea ice motion pattern and sea ice concentration in the Archipelago for the 2002/2003 period (September to June). The

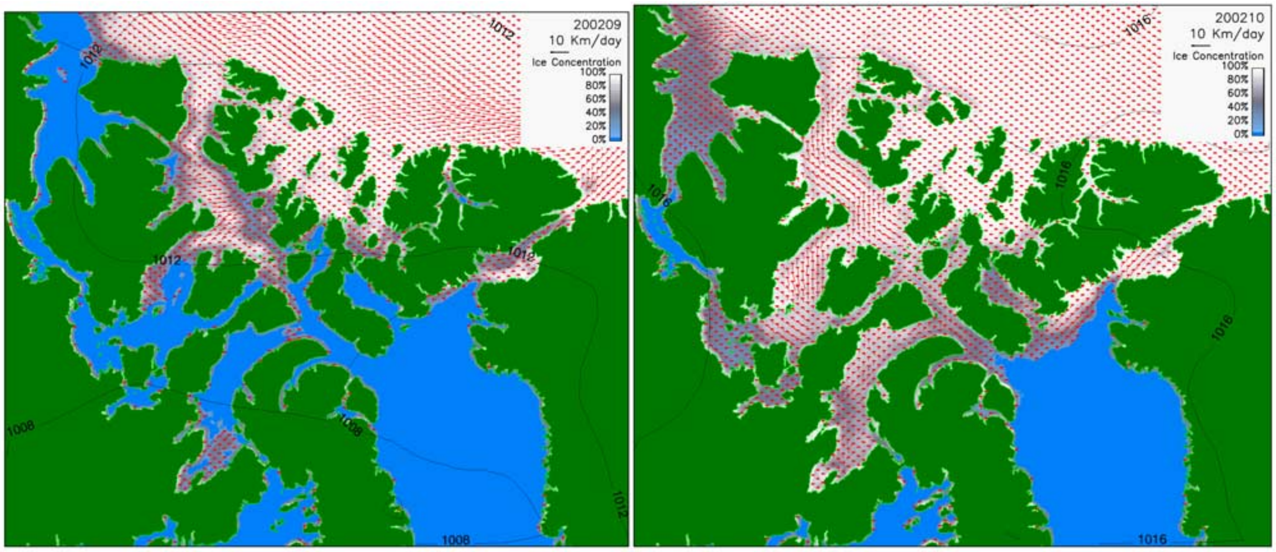

Figure 5a. Monthly average sea ice motion and mean sea level pressure for September and October 2002.

September 2002 graph indicates sea ice still covers MS, QEI-S and QEI-N gates during this month and this is similar for Septembers of other years. The other gates are ice free. The Prince Gustalf Adolf Sea shows a small net monthly sea ice motion of about 3 km/d into the Archipelago while the other gates show little to no ice motion. Other years show small net ice motions across these three gates. In the central part of the Archipelago, most of the sea ice is unconsolidated (mobile). The main channel between M'Clure Strait and Barrow Strait shows net ice motion toward Barrow Strait of about 4 km/d for the month and this is similar for other years. Net ice motion into M'Clintock Channel is about 4 km/d and is similar to other years as well. The main channel from Barrow Strait to Lancaster Sound is largely ice free for September. By October, the Amundsen Gulf gate is ice covered in 3 out of 5 years during this period as is Lancaster Sound. Much of the ice in the central Archipelago is still unconsolidated. The October 2002 pattern of ice motion shows a small net ice export through AG gate. The October of years 2003 and 2004 show a similar but larger export. Net ice motion through the MS gate alternates between years. There is mean ice motion of about 5 km/d through the western part of the main channel from M'Clure Strait to Barrow Strait and southward ice motion into McClintock Channel. In other years the mean monthly ice motion is similar. Especially consistent each year is the southward sea ice motion into M'Clintock Channel. *Howell et al.* [2008] suggests that M'Clintock Channel collects old ice which moves south from the QEI and the consistent southward ice motions each October seem to support this. There is little or no ice motion for the QEI-S and QEI-N gates suggesting that most of this ice is landlocked.

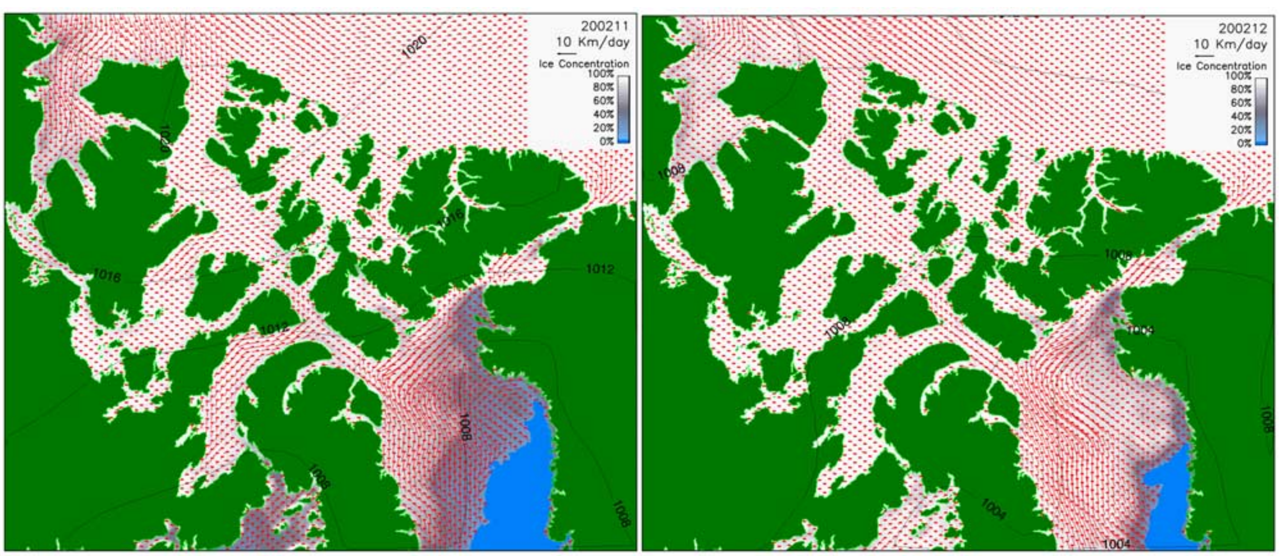

Figure 5b. Monthly average sea ice motion and mean sea level pressure for November and December 2002.

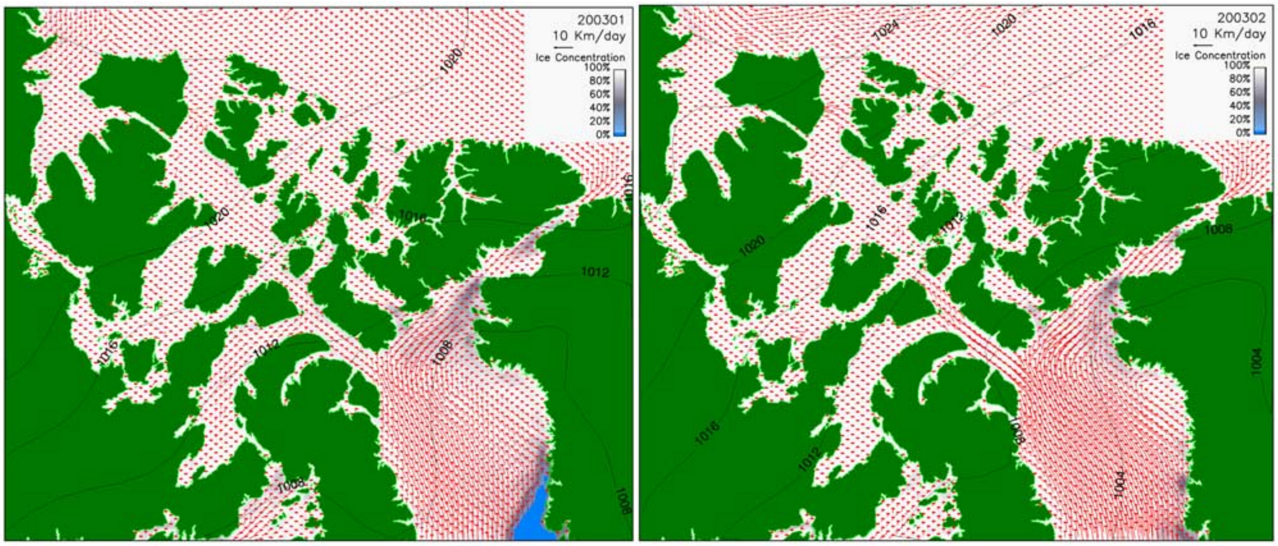

Figure 5c. Monthly average sea ice motion and mean sea level pressure for January and February 2003.

[19] By November (Figure 5b) all gates are ice covered. The November 2002 mean ice motion through the AG and MS gates shows the strongest net export into the Arctic Ocean of any year. In the center of the Archipelago, monthly mean ice motion between M'Clure Strait and Barrow Strait is near zero. This is true for most Novembers except November 2006 when there was a net monthly ice motion toward Barrow Strait of about 3 km/d. There is again a net southward transport of ice into M'Clintock Channel. This also occurred in November 2006 but not in the other 3 years which had no net ice motion for November. The December 2002 ice motion shows a net export of ice out of AG and MS gates. This is similar to other Decembers for the period. Net ice motion in the central Archipelago is negligible indicating that most of the ice in this area is now landfast. The eastern part of Lancaster Sound has a monthly average ice motion of about 5 km/d flowing into strong cyclonic ice motion in northern Baffin Bay. Other Decembers in the period usually show larger ice motions of 7–8 km/d and continue further up the channel to near Barrow Strait. These year to year differences depend on the location of the ice bridge which forms around this time each winter in the Barrow Strait region. The location of the bridge can be inferred from the transition from no net ice motion to the start of ice motion in Lancaster Sound. There is no reduction in the mean ice concentrations since at this time of year, air temperatures are very cold and open ocean freezes over rapidly.

[20] The January 2003 ice motion (Figure 5c) shows sea ice motion through the AG gate into the Beaufort Sea with little ice motion through the other gates facing the Arctic Ocean. In other years there is much smaller ice export through AG gate except 2007 which had the largest ice motions out of the Amundsen Gulf. The central part of the Archipelago shows no ice motion for this month for every year indicating that the central Archipelago remains con-

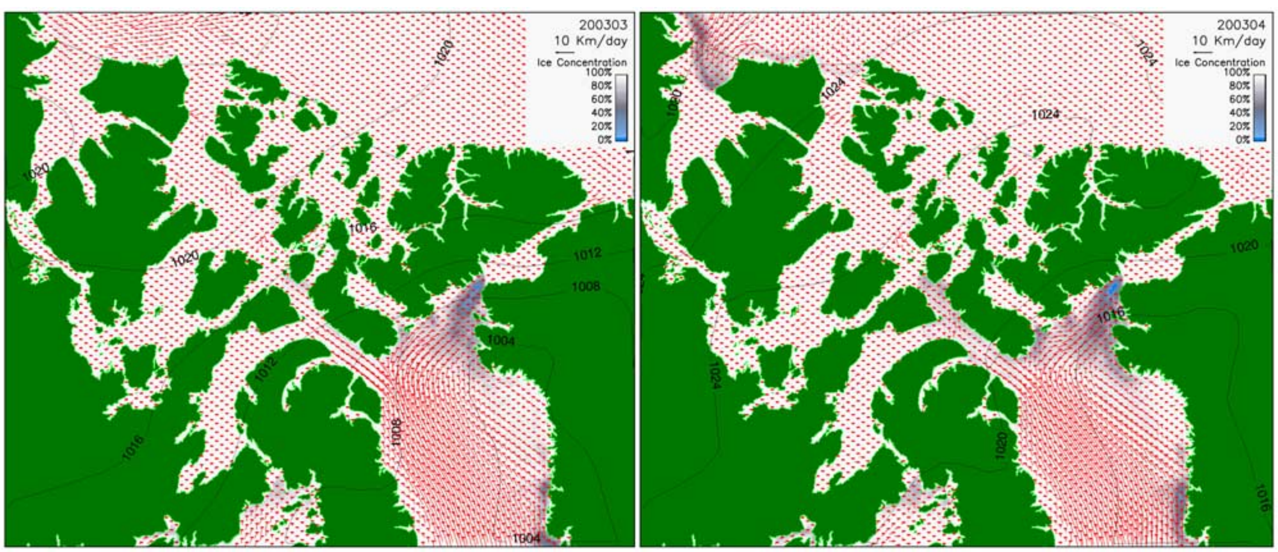

Figure 5d. Monthly average sea ice motion and mean sea level pressure for March and April 2003.

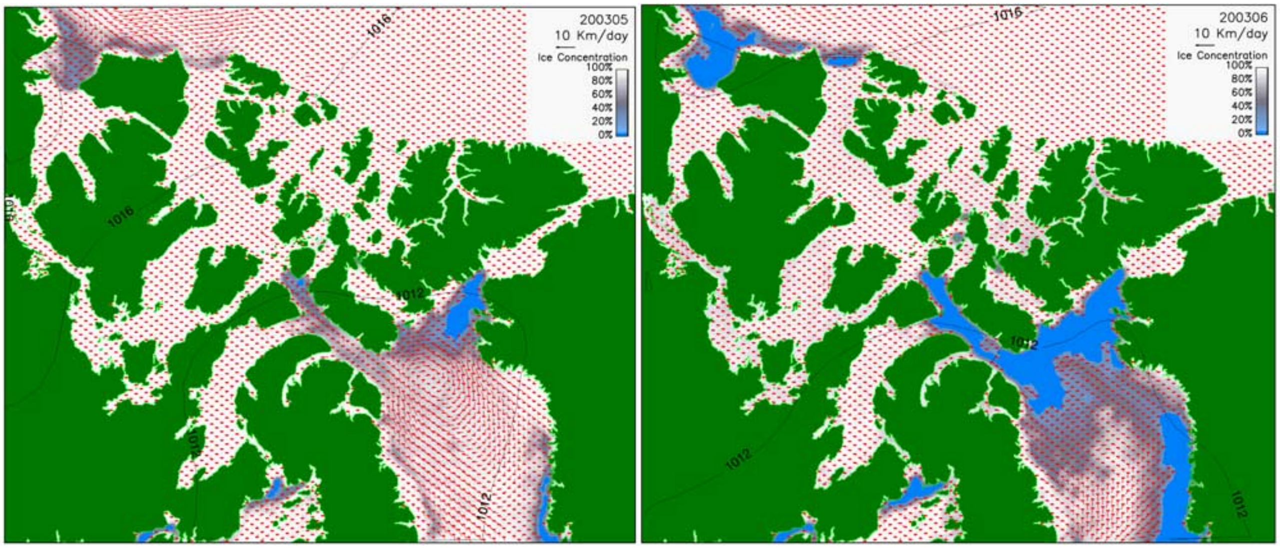

Figure 5e. Monthly average sea ice motion and mean sea level pressure for May and June 2003.

solidated. Ice motion in Lancaster Sound downstream from the ice bridge is eastward toward Baffin Bay at about 4 km/d. Most other years showed stronger net ice motions around 7 km/d toward Baffin Bay. February 2003 shows a small net ice export into the Beaufort Sea through the AG gate. Other years have a similar small net export. There is little net ice motion in the Archipelago itself except for Barrow Strait and Lancaster Sound which had mean eastward ice motion ranging from 8 to 10 km/d. Other years show a similar monthly pattern. All years show strong southeasterly ice motions of 10 to 15 km/d in northern Baffin Bay for this month. The March 2003 net ice motion (Figure 5d) shows little or no net export of ice through AG gate except for March 2005 which had mean ice export across the gate of about 3 km/d. Lancaster Sound continues to show strong eastward ice motions feeding into the strong southeasterly transport of ice in Baffin Bay. The April 2003 image shows ice motion into the Beaufort Sea with little motion for the other gates facing the Arctic Ocean. This is similar for other years. Reduced sea ice concentration in Amundsen Gulf indicates that sea ice formation after a lead opens up is not occurring or not occurring quickly enough. This shows up in reduced sea ice concentrations. Eastward transport of ice in Lancaster Sound continued, although the mean ice motion is reduced. Southward transport of sea ice in Baffin Bay continued and reduced mean sea ice concentration in northern Baffin Bay reveals the location of the North Open Water polynya.

[21] The May 2003 ice concentration pattern (Figure 5e) shows more regions of frequent leads and polynya formation in Amundsen Gulf, Lancaster Sound and the very northern part of Baffin Bay. The AG gate continues to export ice into the Beaufort Sea and this is true for other years as well. There is no ice motion in the central part of the Archipelago which is still landfast. Lancaster Sound continues to export sea ice into Baffin Bay. The strong cyclonic ice motion in Baffin Bay was observed every year. The June 2003 ice motion and concentration pattern shows more open water in the region of the AG and MS gates with little or no net ice motion in the interior of the Archipelago. The Lancaster Sound and North Open Water polynyas are beginning to merge and the mean southward transport of ice in Baffin Bay is reduced.

3.3. Monthly Average Fluxes Across the Gates for the 2002 to 2007 Period

[22] Monthly sea ice area fluxes for each gate and each year are shown in Figure 6 and the 10-month average ice area flux (September to June) is shown in Table 3. The table shows that the AG gate had an average export of sea ice area of -42×10^3 km^2 a^{-1} (into the Arctic Ocean) ranging from -77 to -20×10^3 km^2. MS gate had an average ice area export of -12×10^3 km^2 ranging from -39 to $+1 \times 10^3$ km^2. The graph for the AG and MS gate in Figure 6 show considerable monthly variability from year to year especially in the fall and early winter months (October, November, December and January). This reflects the higher mobility of the ice at this time and the strength and location of the Beaufort Sea anti-cyclonic circulation which intensifies at this time of year [*Barber and Hanesiak*, 2004]. QEI-S and QEI-N gates had no net ice flux for the 5-year period (Table 3) and variability from year to year ranged from -10 to $+8 \times 10^3$ km^2 considerably lower than the AG and MS gates. It should be kept in mind that these two gates are ice covered in July and August when no flux estimates were available and when much of the sea ice in the lower part of the QEI has melted providing a southward escape route for ice in the vicinity of these gates. *Alt et al.* [2006] has investigated sea ice conditions in the QEI region between 1998 and 2005 after the record low ice cover in the summer of 1998 and has found evidence that pack ice from the Arctic Ocean has moved into the QEI region in the summer of 2005.

[23] The Arctic Oscillation is defined as the first EOF of the mean sea level pressure (slp) over the Northern Hemisphere [*Thompson and Wallace*, 2001]. *Rigor et al.* [2002], *Rigor and Wallace* [2004], and others show a strong correlation between sea ice motion over the Arctic Ocean and the Arctic Oscillation Index (AO). Correlation with the monthly AO index and monthly ice export through AG and MS gates was +0.48 and +0.40 which are low but still significantly different from zero at the $p = 0.05$ level. They are positively correlated

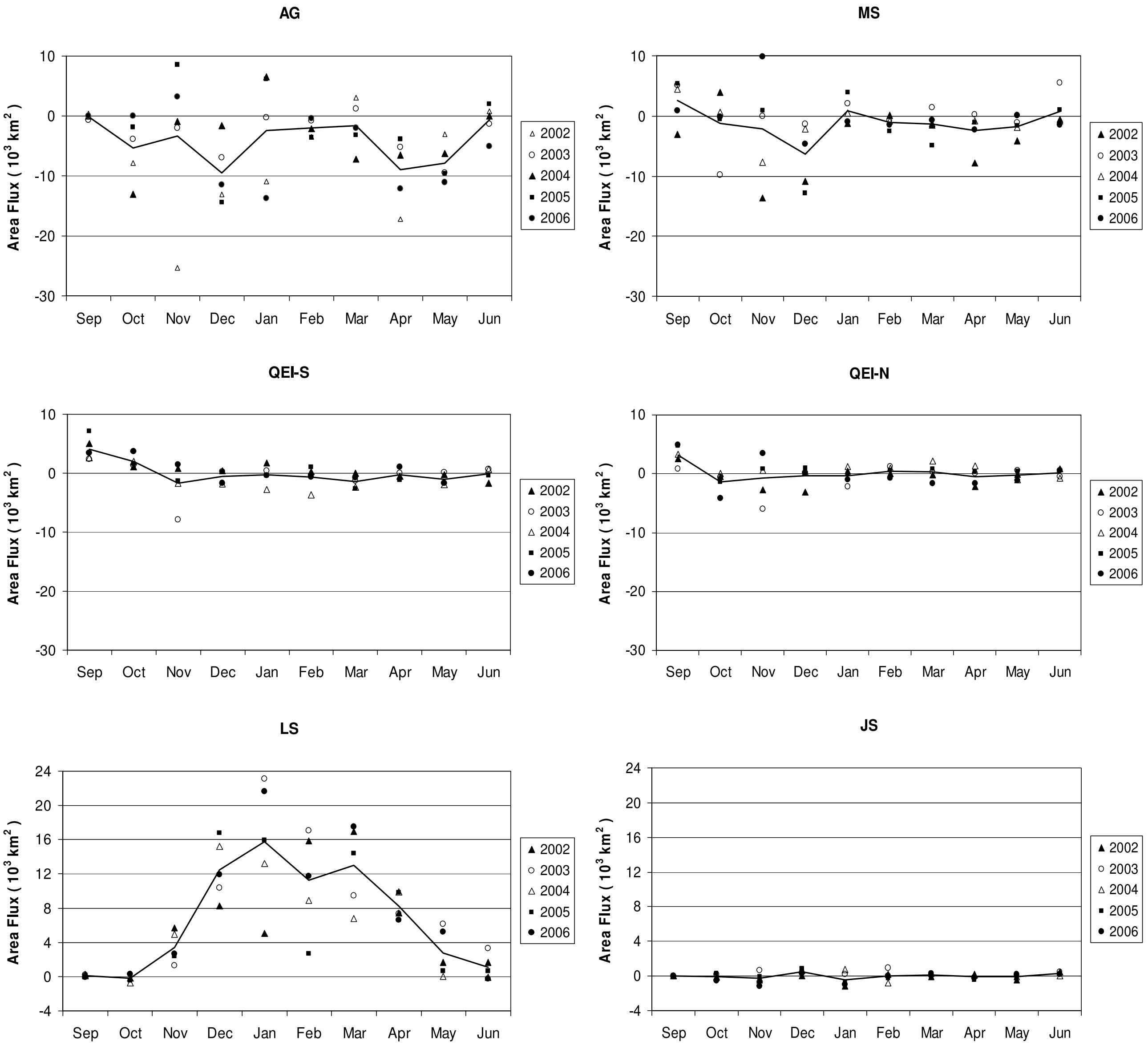

Figure 6. Monthly sea ice area flux by year for AG gates, MS gate, QEI-S gate, QEI-N gate, LS gate, and JS gate. Years are labeled according to the September of the year. The solid line in each graph is the 5-year monthly average for each gate.

indicating that low AO index which corresponds to a strong Beaufort Sea high pressure and gyre is associated with more ice export into the Arctic Ocean. These correlations are not strong and may reflect the fact that ice motions through these gates are regional and confined to the nearshore of the Beaufort Sea where coastal effects are important, whereas the AO is a broad index of atmospheric circulation over the entire Arctic Ocean. The Dipole Anomaly index [*Wu et al.*, 2006] is the second EOF of the slp accounting for regional differences in pressure between the Eurasian and North American side of the Arctic Ocean. It has been shown to influence regional sea ice motion. However, monthly estimates of the Dipole Anomaly are not available (J. Wang, private communication) and calculating it from the NCEP reanalysis is beyond the scope of this paper. The correlation of the AO index with ice flux from QEI-S and QEI-N gates was not significant.

[24] The LS gate had an average yearly ice area export of 68 $\times$ 10^3 km^2 into Baffin Bay ranging from 77 to 58 $\times$ 10^3 km^2 for this 5-year period (Table 3). Monthly averages were positive in almost every month.

Table 3. Cumulative 10-Month Sea Ice Area Fluxes for Gates Facing the Arctic Ocean and Facing Baffin Bay[a]

Year	AG	MS	QEI-S	QEI-N	LS	JS
2002/2003	−77	−39	7	−5	63	−1
2003/2004	−29	1	−4	−6	79	3
2004/2005	−31	−10	−10	8	58	1
2005/2006	−20	−12	2	8	63	0
2006/2007	−53	−1	4	−1	77	−2
Average	−42	−12	0	0	68	0
Estimated ice thickness (m)	1	2.5	3.4	3.4	1.5	1.5
Volume flux (km^3)	−42	−30	0	0	102	0

[a]Units are in 10^3 km^2 a^{-1}.

Correlation with the monthly AO index was −0.33 and not significant. Because the LS gate is on the western edge of Baffin Bay, it is more under the influence of large scale atmospheric circulation in the north Atlantic. The correlation of ice area flux through the LS gate and the North American Oscillation (NAO) index [*Rogers and van Loon*, 1979] was 0.40 and was significant at the p = 0.05 level. The correlation is positive indicating that high NAO index (a strong southerly flow in Baffin Bay and deep Icelandic Low) corresponds to increased ice export into Baffin Bay. The JS gate ice area flux contribution was negligible in comparison and had no net yearly ice area flux for the period and no significant correlation with the AO or NAO index.

[25] Estimates based on Kwok's RADARSAT analysis for the 6-year period preceding this study are in general agreement with these results. For the AG and MS gates, he found a slightly higher ice export of -85×10^3 km^2 and -20×10^3 km^2 a^{-1}. He also found a net ice import through QEI-S and QEI-N of 6×10^3 km^2 and 2×10^3 km^2, respectively. These differences may result from ice flux estimates missing for July and August in this study. Also there is large yearly variability in atmospheric circulation and ice conditions in the Archipelago from year to year. In particular, the record low ice concentrations in the Archipelago in the summer of 1998 [*Jeffers et al.*, 2001] would have conditioned the ice to allow influx of pack ice from the Arctic Ocean in following years. There is some suggestion that this occurred as part of the recovery of the ice regime after the summer of 1998 [*Alt et al.*, 2006]. Older thick ice, once re-established, would resist import of pack ice from the Arctic Ocean through the QEI.

[26] As mentioned earlier, ice volume flux estimates require daily ice thickness data along each gate. These are not available. However, a rough estimate of average ice thickness can be made based on the sea ice climatology surrounding each gate. It should be kept in mind that these volume flux estimates are very approximate. For the AG gate, the *Canadian Arctic Shelf Exchange Study* (*CASES*) [2004] which summarizes ice types in Amundsen Gulf was used. Across this gate, the Cape Bathurst polynya often forms and as a result a wide range of ice types from nilas to thick first year ice pass the AG gate over the winter. Based on this, an average ice thickness of 1 m is used to produce a rough estimate of ice volume export of −42 km^3 a^{-1}. For the M'Clure Strait gate the *Annual Arctic Sea Ice Atlas* [2006] from Environment Canada is used. Sea ice in M'Clure Strait is mainly a combination of first-year and multiyear ice. Based on this, a reasonable estimate of ice thickness is 2.5 m producing a volume flux of −30 km^3 a^{-1} into the Beaufort Sea. Based on data from mooring sites in Lancaster Sound and S. Prinsenberg (private communication), a rough estimate of the thickness of sea ice passing the LS fluxgate and JS fluxgate is 1.5 m. This produces an average ice volume flux of 112 km^3 a^{-1} for a total volume export into Baffin Bay. Adding all these fluxes, the Archipelago exports a total of roughly 174 km^3 of sea ice into both the Arctic Ocean and Baffin Bay.

4. Conclusions

[27] Enhanced resolution AMSR-E imagery can be used to estimate sea ice motion and sea ice area fluxes in the main channels of the Canadian Archipelago. This imagery has better daily repeat coverage compared to RADARSAT which has repeat coverage about every three days for this region. However, the spatial resolution of the enhanced AMSR-E imagery is coarser and increased atmospheric absorption in summer prevents estimating ice motion in July and August using the 89 GHz channels. Enhanced AMSR-E data extends the capability of monitoring ice motions in the Canadian Archipelago to another sensor and extends the baseline of sea ice flux estimates for the northern channels 5 more years from September 2002 to June 2007. Extending the record helps remove aliasing caused by the exceptionally light 1998 ice year in the region. This database of daily ice motions in the Archipelago and northern Baffin Bay are available for regional climate modeling evaluation and testing and will eventually become part of the Canadian Cryospheric Information Network (http://www.ccin.ca/).

[28] This study found that the largest daily fluxes and flux variability occurs through Amundsen Gulf and M'Clure Strait gates facing the Arctic Ocean and through Lancaster Sound gate facing Baffin Bay. Daily fluxes as large as ±2500 km^2 can occur and are event driven as weather systems move through the region. Averaged over this 5-year period, AG and MS gates had a net export of 42×10^3 km^2 and 12×10^3 km^2 of sea ice area into the Arctic Ocean. Although no net flux through the Queen Elizabeth Island gates (QEI-S and QEI-N) was found, it should be kept in mind that both these gates are ice covered during July and August when no sea ice flux estimates were made. The LS gate frequently exported sea ice into Baffin Bay with occasional reversal determined mainly by changes in large scale circulation. Averaged over the period, there was a net sea ice export of 68×10^3 km^2 a^{-1} into Baffin Bay. JS gate had no net transport over the period.

[29] Net fluxes into both the Arctic Ocean and Baffin Bay resulted in a net loss of sea ice for the Archipelago of about 122×10^3 km^2 of sea ice area or roughly 174 km^3 of ice volume each year. This sea ice is presumably generated within the Canadian Archipelago itself, mainly through the large number of stationary and transient polynyas and leads which form over the winter. These fluxes are small compared to the southward transport of sea ice area in Baffin Bay (530×10^3 km^2) and through Fram Strait (900×10^3 km^2) [*Kwok*, 2007; *Kwok and Rothrock*, 1999].

[30] The msl pressure difference across each gate is a fair predictor of flux and the correlations range from 0.60 for the AG gate to 0.40 for the QEI-N gate. However, near these gates internal ice stresses caused by local sea ice interaction can be large and free ice drift conditions will not always exist. Cross-gradient flux relationships for the LS gate show a large number of counter gradient ice fluxes suggesting that local mesoscale winds (nongeostrophic) and perhaps ocean currents play a role in transporting sea ice through this gate. Monthly fluxes for the AG and MS gates were positively correlated with the AO index indicating that a strong Beaufort Sea high pressure and gyre correspond to more export into the Beaufort Sea. Monthly fluxes for the LS gate were positively correlated with the NAO index indicating that strong southerly flow in Baffin Bay increases ice export into Baffin Bay.

[31] **Acknowledgments.** The authors would like to thank Linda Enciu for her assistance during preparation of the manuscript. The authors acknowledge the National Snow and Ice Data Center for providing the AMSR-E data products and the International Arctic Buoy Program for providing the Arctic buoy data. This work is partially funded by the Canadian Panel on Energy Research and Development (PERD) and a U.S. National Science Foundation grant OPP-0230236 and is an element of the Arctic-Subarctic Ocean Flux (ASOF) program supported by the NSF Office of Polar Programs grant OPP-0230382.

References

Agnew, T. A., H. Le, and T. Hirose (1997), Estimation of large scale sea ice motion from SSM/I 85.5 GHz imagery, *Ann. Glaciol.*, *25*, 305–311.

Alt, B., K. Wilson, and T. Carrieres (2006), A case study of old ice import and export through the Peary and Sverdrup Channels of the Canadian Arctic Archipelago, *Ann. Glaciol.*, *44*, 329–338.

Annual Arctic Sea Ice Atlas (2006), *Winter 2006 includes 2005/2004/2003, Can.* Ice Serv., Environ. Can., Ottawa, Ont., Canada.

Barber, D. G., and J. M. Hanesiak (2004), Meteorological forcing of sea ice concentrations in the southern Beaufort Sea over the period 1979 to 2000, *J. Geophys. Res.*, *109*, C06014, doi:10.1029/2003JC002027.

Canadian Arctic Shelf Exchange Study (CASES) (2004), *Ice-atmosphere interactions and biological linkages, data report, sub-group 2.2,* CEOS-TEC-2004–09–01, Cent. for Earth Obs. Sci., Dep. of Geogr., Univ. of Manitoba, Winnipeg, Manitoba, Canada.

Cavalieri, D., and G. Crawford (1991), Aircraft active and passive micro validation of sea ice concentration from DSMP SSMI, *J. Geophys. Res.*, *96*(C12), 21,989–22,008.

Cavalieri, D., C. Parkinson, and P. Gloersen (1999), Deriving long-term time series of sea ice cover from satellite microwave multisensor data sets, *J. Geophys. Res.*, *104*(C7), 15,803–15,814.

Early, D. S., and D. G. Long (2001), Image reconstruction and enhanced resolution imaging from irregular samples, *IEEE Trans. Geosci. Remote Sens.*, *39*, 291–302.

Howell, S. E. L., A. Tivy, J. J. Yackel, and S. McCourt (2008), Multi-year ice conditions in the western CAA Region of the NWP: 1968–2006, *Atmos. Ocean*, *46*(2), 229–242.

Jeffers, S., T. A. Agnew, B. T. Alt, R. De Abreu, and S. McCourt (2001), Investigating the anomalous sea ice conditions in the Canadian High Arctic (Queen Elizabeth Islands) during the summer of 1998, *Ann. Glaciol.*, *33*, 507–512.

Jones, E. P., J. H. Swift, L. G. Anderson, M. Lipizer, G. Civitarese, K. K. Falkner, G. Kattner, and F. McLaughlin (2003), Tracing Pacific water in the North Atlantic Ocean, *J. Geophys. Res.*, *108*(C4), 3116, doi:10.1029/2001JC001141.

Kwok, R. (2006), Exchange of sea ice between the Arctic Ocean and the Canadian Arctic Archipelago, *Geophys. Res. Lett.*, *33*, L16501, doi:10.1029/2006GL027094.

Kwok, R. (2007), Baffin Bay ice drift and export: 2002–2007, *Geophys. Res. Lett.*, *34*, L19501, doi:10.1029/2007GL031204.

Kwok, R., and D. Rothrock (1999), Variability of Fram Strait ice flux and North Atlantic Oscillation, *J. Geophys. Res.*, *104*(C3), 5177–5189.

Kwok, R., A. Schweiger, D. A. Rothrock, S. Pang, and C. Kottmeier (1998), Sea ice motion from satellite passive microwave imagery assessed with ERS SAR and buoy motions, *J. Geophys. Res.*, *103*, 8191–8214.

Kwok, R., G. F. Cunningham, H. J. Zwally, and D. Yi (2007), ICESat over Arctic sea ice: Retrieval of freeboard, *J. Geophys. Res.*, *112*, C12013, doi:10.1029/2006JC003978.

Long, D., and D. Daum (1998), Spatial resolution enhancement of SSM/I data, *IEEE Trans. Geosci. Remote Sens.*, *36*(2), 407–417.

Marko, J. (1982), The ice environment of eastern Lancaster Sound and Northern Baffin Bay, in Indian and Northern Affairs, *Environ. Stud.*, *26*, 1–215.

Meier, W., J. Stroeve, and F. Fetterer (2007), Whither Arctic sea ice? A clear signal of decline regionally, seasonally, and extending beyond the satellite record, *Ann. Glaciol.*, *46*, 428–434.

Melling, H. (2002), Sea ice of the northern Canadian Arctic Archipelago, *J. Geophys. Res.*, *107*(C11), 3181, doi:10.1029/2001JC001102.

Melling, H., T. Agnew, K. Kalkner, D. Greenberg, C. Lee, A. Muchow, B. Petrie, S. Prinsenberg, R. Samelson, and R. Woodgate (2008), Freshwater fluxes via Pacific and Arctic outflows cross the Canadian polar shelf, in *Arctic-Subarctic Ocean Fluxes: Defining the Role of the Northern Seas in Climate*, edited by B. Dickson and P. Rhines chap. 9, Springer, New York.

Ngheim, S. V., Y. Choa, G. Neumann, P. Li, D. K. Perovich, T. Street, and P. Clemente-Colon (2006), Depletion of perennial sea ice in the East Arctic Ocean, *Geophys. Res. Lett.*, *33*, L17501, doi:10.1029/2006GL027198.

Prinsenberg, S., and J. Hamilton (2005), Monitoring the volume, freshwater and heat fluxes passing through Lancaster Sound in the Canadian Arctic Archipelago, *Atmos. Ocean*, *43*(1), 1–22.

Rigor, I. G., and J. Wallace (2004), Variations in the age of Arctic sea ice and summer sea ice extent, , *Geophys. Res. Lett.*, *31*, L09401, doi:10.1029/2004GL019492.

Rigor, I. G., J. M. Wallace, and R. L. Colony (2002), On the response of sea ice to the Arctic Oscillation, *J. Clim.*, *15*, 2648–2663.

Rogers, J. C., and H. van Loon (1979), The seesaw in winter temperatures between Greenland and northern Europe. Part I. General description, *Mon. Weather Rev.*, *107*, 296–310.

Samelson, R. M., T. Agnew, H. Melling, and A. Munchow (2006), Evidence for atmospheric control of sea-ice motion through Nares Strait, *Geophys. Res. Lett.*, *33*, L02506, doi:10.1029/2005GL025016.

Smith, S. D., R. D. Muench, and C. H. Pease (1990), Polynyas and leads: An overview of physical processes and environment, *J. Geophys. Res.*, *95*(C6), 9461–9479.

Spreen, G., S. Kern, D. Stammer, R. Forsberg, and J. Haarpaintner (2006), Satellite-based estimates of sea ice volume flux through Fram Strait, *Ann. Glaciol.*, *44*, 321–328.

Stroeve, J., M. Holland, W. Meier, T. Scambos, and M. Serreze (2007), Arctic sea ice decline: Faster than forecast, *Geophys. Res. Lett.*, *34*, L09501, doi:10.1029/2007GL029703.

Thompson, D. W. J., and J. M. Wallace (2001), Regional climate impacts of the Northern Hemisphere annular mode, *Science*, *293*, 85–89.

Thorndike, A. S., and R. Colony (1982), Sea ice motion in response to geostrophic winds, *J. Geophys. Res.*, *87*(C8), 5845–5852.

Wilson, K. J., J. Kalkingham, H. Melling, and R. A. de Abreu (2004), Shipping in the Canadian Arctic: Other possible climate change scenarios, paper presented at International Geoscience and Remote Sensing Symposium (IGARSS 2004), Anchorage, Alaska, 20–24 Sept.

Wu, B., J. Wang, and J. E. Walsh (2006), Dipole anomaly in the winter Arctic atmosphere and its association with ice motion, *J. Clim.*, *19*, 210–225.

T. Agnew, Environment Canada, 4905 Dufferin Street, Toronto, ON M3H 5T4, Canada. (tom.agnew@ec.gc.ca)

A. Lambe, Faculty of Applied Science and Engineering, University of Toronto, 40 St. George Street, Toronto, ON M5S 2E4, Canada. (andrew.lambe@utoronto.ca)

D. Long, Microwave Earth Remote Sensing Laboratory, Brigham Young University, 459 Clyde Building, Provo, UT 84601, USA. (long@byu.edu)